# The mechanism study of *Eag1* potassium channel in gastric cancer

**Shan Gao[1#]^, Wei Wang[1#]^, Wanqing Ye[2,3]^, Ke Wang[2,3]^**

[1]Department of Gastroenterology, Xiangyang Central Hospital, Affiliated Hospital of Hubei University of Arts and Science, Xiangyang, China; [2]Department of Preventive Medicine, Medical College, Hubei University of Arts and Science, Xiangyang, China; [3]Center for Clinical Evidence-Based and Translational Medicine, Xiangyang Central Hospital, Affiliated Hospital of Hubei University of Arts and Science, Xiangyang, China

*Contributions:* (I) Conception and design: S Gao, W Wang, K Wang; (II) Administrative support: K Wang, S Gao; (III) Provision of study materials or patients: All authors; (IV) Collection and assembly of data: W Wang, W Ye; (V) Data analysis and interpretation: W Wang, K Wang; (VI) Manuscript writing: All authors; (VII) Final approval of manuscript: All authors.

[#]These authors contributed equally to this work.

*Correspondence to:* Ke Wang. Department of Preventive Medicine, Medical College, Hubei University of Arts and Science, 296 Longzhong Road, Xiangyang 441053, China. Email: mqlhome76@163.com.

**Background:** Heredity factors may play a vital role in gastric cancer (GC) progression. This study is aimed to explore and validate the influence and the role of *Eag1* on the susceptibility to GC.

**Methods:** The successfully constructed Ad5-Eag1-shRNA vector was transfected into GC cells [SGC-7901 and BGC-823, short hairpin RNA (shRNA) group]. Reverse transcription polymerase chain reaction (RT-PCR) and western blotting were conducted for assessment of *Eag1* messenger RNA (mRNA) and protein expression levels. Cell proliferation and cell colony formation was measured by Cell Counting Kit-8 (CCK-8) assays. Flow cytometry was performed for cell cycle progression assessment. Bioinformatic analysis was analyzed for *Eag1* validation with multiple public databases.

**Results:** The expression of *Eag1* was significantly down-regulated in the shRNA group in comparison with the empty vector and control groups (P<0.05). Cell proliferation rate and clone formation number were lower in the shRNA group, and a decreased cell proportion in $G_2$-S phase and an increased proportion in $G_1$-$G_0$ were observed in the shRNA group (P<0.05). When transfected with Ad5-Eag1-shRNA, cyclin D1 and cyclin E protein expression were inhibited. Bioinformatic analysis showed that *Eag1* expression was strongly associated with the prognosis and immune infiltration of GC.

**Conclusions:** The *Eag1* gene may affect occurrence and development of GC through regulating cyclin D1 and cyclin E expression.

**Keywords:** *Eag1* channel; gastric cancer (GC); cell apoptosis; biological function; bioinformatic analysis

## Introduction

Gastric cancer (GC) is a key reason for cancer morbidity and mortality worldwide, accounting for more than 1080,000 incidences every year and an estimated 768,000 deaths in 2020 (1,2). Although treatment and diagnosis of GC have been improved recently, the 5-year overall survival (OS) rate is still relatively low (3). As a result, GC has become a major contributor to the burden of cancer, accounting for 20% worldwide, following lung

^ ORCID: Shan Gao, 0000-0001-9559-3280; Wei Wang, 0000-0001-9756-1821; Wanqing Ye, 0000-0001-6098-1232; Ke Wang, 0000-0003-0829-8510.

and liver cancer (4). As a kind of heterogeneous disease, GC regulation can be affected by heredity and complex molecular mechanisms (5). Several reports have shown that heredity can affect cancer progression, accounting for 10% of GC cases (6,7). Therefore, exploring the specific molecular markers for biological mechanism exploration of GC is important and urgent.

The abnormal regulation of key genes in potassium channels has been found in several kinds of cancer. Among these potassium channels, voltage-gated ether à-go-go-1 (*Eag1*) has received more attention for tumor pathogenesis in recent years because of its close relation with cell proliferation, survival, angiogenesis, migration, and invasion of cancer cells (8-10). Interestingly, higher expression of *Eag1* has been found in most human tumors than in normal tissues (11,12). Further, abnormal expression of *Eag1* has been reported to result in a strong immune response in breast cancer (13,14). Moreover, many biological studies have provided strong evidence of the importance of *Eag1* in tumor development (15,16). Hence, this attractive feature of restricted expression in normal tissues suggests that *Eag1* may be a useful individualized marker in tumor diagnosis, mechanism research and targeted drug therapy. To date, few studies have reported the effect of *Eag1* expression on the oncogenic potential in GC.

The objective of this study was to explore and validate the influence and the role of *Eag1* channel on the susceptibility to GC. The relationship between *Eag1* expression and cell biology was analyzed in GC cells. Biological experiments were performed to estimate the influence of *Eag1* knockdown on cell function. Bioinformatics analysis was analyzed for *Eag1* validation with multiple public databases. We also further evaluated the influence of different *Eag1* expression levels on cyclin D1 as well as cyclin E to explore GC progression. We present the following article in accordance with the MDAR reporting checklist (available at https://tcr.amegroups.com/article/view/10.21037/tcr-22-2276/rc).

## Methods

### Cell culture

The GC cell lines SGC-7901 and BGC-823 were provided and identified by American Type Culture Collection (ATCC; Manassas, VA, USA). Cells with a passage time less than 6 months were used in this study. Fetal bovine serum (FBS; Invitrogen, Carlsbad, CA, USA) was used to culture GC

cell lines, including 10% FBS and 5% 0.1 mM penicillin-streptomycin in the environment of 5% $CO_2$ at 37 ℃.

### Vector construction

Knockdown vectors were generated by using adenovirus following the instructions; GC cells in the exponential growth period were collected and infected with the adenovirus vector containing *Eag1* short-hairpin RNAs (shRNAs) or an empty vector. Western blotting was conducted to validate whether the knockdown of *Eag1* and empty vector were satisfactory, and then fresh medium was provided for stable cell culture. The sequences for the *Eag1* shRNAs were as shown: target 1 (GCGGTCCAATGATACTAAT), target 2 (CCATCTTGGTCCCTTATAA), and target 3 (CAAACTTATCCGCATGAAC).

### RNA extraction and reverse transcription polymerase chain reaction (RT-PCR)

Total cell RNA was extracted according to manufacturer's instructions of TRIzol reagent (Invitrogen, Shanghai, China). Reverse transcription of total RNA was conducted under standard conditions in 10 µl volume with PrimeScript RT Reagent Kit (TaKaRa, Dalian, China). SYBR Green real-time polymerase chain reaction (PCR) was used to measure gene expression of *Eag1*. The messenger RNA (mRNA) expression level of *Eag1* was estimated by the $2\times2^{-\Delta\Delta Ct}$ method, taking glyceraldehyde 3-phosphate dehydrogenase (GAPDH) as a reference. The specific primer sequences of *Eag1* were as follows: (F) 5'-AGAACGTGGATGAGGGCATCAG-3', (R) 5'-ACTGGTAAGGGGTGCCAATG-3'. The primers for GAPDH were (F) 5'-TCAAGAAGGTGGTGAAGCAGG-3' and (R) 5'-TCAAAGGTGGAGGAGTGGGT-3'. Quantitative (q)PCR assays and a LightCycler 480 instrument (Roche, Basel, Switzerland) were utilized to collect the data.

### Protein extraction and western blotting

The GC cell lines cultured in the logarithmic growth phase were collected for protein extraction. After transfection for 48 hours, GC cells were treated with cell lysis buffer for 30 minutes and boiled for 10 minutes for denaturation. Electrophoresis in 12% polyacrylamide gels was performed with 40 µg of protein in each sample.

In this way, the protein was successfully transferred to polyvinylidene fluoride (PVDF) membranes (Millipore, Burlington, MA, USA) and then soaked in tris-buffered saline with Tween 20 (TBST) blocking buffer including 5% skim milk powder and blocked for 2 hours. Antibodies against Eag1, GAPDH, cyclin D1 and cyclin E were incubated overnight at 4 ℃. With washing 5 times in TBST, PVDF membranes were then incubated in the secondary antibody solution with a dilution of 1:50,000 for 2 hours at 37 ℃. An electrochemiluminescence (ECL) detection kit was used to detect the immunoreactive protein bands. The gray values of protein bands were scanned and analyzed by Azure c300 Gel Imaging System (Azure Biosystems, Dublin, USA). Each independent experiment was repeated 3 times.

### Cell proliferation and cell colony

Cell lines cultured in logarithmic growth phase were inoculated in 96-well plates. After culturing for 12 hours with serum-free 1640 medium, the GC cells were transfected with Eag1-shRNA and Eag1-shRNA-NC (empty vector). The transfected cells were mixed with 10 μL of cholecystokinin octapeptide (CCK-8; Biosharp, Hefei, China) solution and incubated for another 4 hours at 37 ℃. A microplate reader with the absorbance of 450 nm was used for cell detection.

Clone formation was performed in transfected cells (Eag1-shRNA and empty vector), which were cultured for 3 weeks at 37 ℃ in the presence of 5% $CO_2$. After dropping the culture solution and fixing with 4% methanol for 15 minutes, the plates were stained with iodonitrotetrazolium (INT; Sigma, St. Louis, MO, USA). The number of colonies was counted by microscopic observation. Cloning efficiency was defined as the number of cell colonies/ inoculated cell number ×100%.

### Cell apoptosis and cell-cycle progression

Cell lines were transfected for 48 hours with Annexin V-APC and 7-AAD and then collected for testing. The information of cell apoptosis and cell cycle progression was measured by flow cytometry [Becton, Dickinson, and Co. (BD) Biosciences, Franklin Lakes, NJ, USA]. Cell Quest software (BD Biosciences) was used to evaluate the time phase distribution of the cell cycle. Cells were divided into 3 types (viable cells, apoptotic cells, and dead cells) according to their state. Each sample was assayed 3 times.

### mRNA and protein expression validation

The difference of *Eag1* gene expression in tumor sample and normal sample was validated in The Cancer Genome Atlas (TCGA) database. Immunohistochemistry information was provided by The Human Protein Atlas (HPA), in both tumor sample and adjacent normal sample of GC cases. The study was conducted in accordance with the Declaration of Helsinki (as revised in 2013).

### Functional enrichment analysis

A Volcano plot and heatmap were used to evaluate the differentially expressed genes (DEGs) of *Eag1*. Functional enrichment analysis including Gene Ontology (GO) and Kyoto Encyclopedia of Genes and Genomes (KEGG) were used for molecular biological functions estimation. Biological processes (BPs), cellular components (CCs), and molecular functions (MFs) were assessed respectively.

### Relationship between Eag1 expression and immune infiltration

The relationship between *Eag1* expression level and immune infiltration in cancer-associated fibroblasts, T cells, and neutrophils was analyzed by Tumor Immune Estimation Resource version 2 (TIMER2; http://timer.cistrome. org/). The Tumor-Immune System Interaction Database (TISIDB; http://cis.hku.hk/TISIDB/) was conducted to estimate the relationship between *Eag1* expression level and abundance of immune cells. Spearman correlation coefficient was calculated for evaluation.

### Statistical analysis

The characteristics of continuous variables were presented as the mean ± standard deviation (SD). To compare the difference between two groups, either Student's *t*-test or Mann-Whitney U test was performed. One-way analysis of variance (ANOVA) was analyzed to calculate difference of means among more than two groups. Kaplan-Meier survival analysis was used for subgroup analysis of *Eag1* gene expression level and GC prognosis. Then, a nomogram was performed with *Eag1* expression and some clinicopathological variables. A two-sided P value less than 0.05 was defined as a statistically significant difference. Graphics were drawn by R software (R 3.6.1; The R Foundation for Statistical Computing, Vienna, Austria)
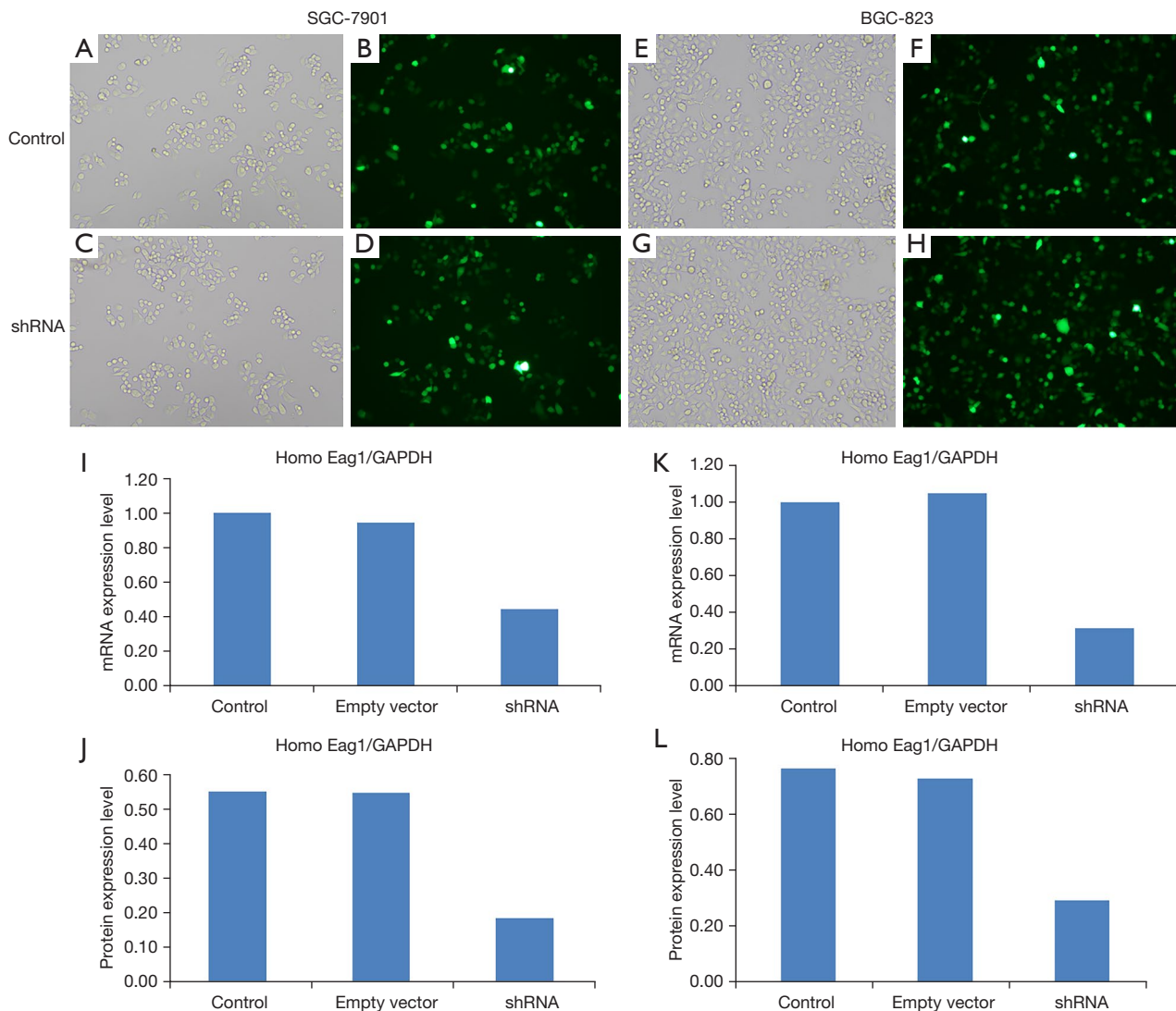
**Figure 1** Effects of transfection and *Eag1* knockdown on gastric cancer cell viability *in vitro*. (A,C) Transfection efficiency of Ad5-Eag1-shRNA in light microscopic pictures of SGC-7901. (B,D) Fluorescent microscopic pictures of SGC-7901 with GFP expression vector. (E,G) Transfection efficiency of Ad5-Eag1-shRNA in light microscopic pictures of BGC-823. (F,H) Fluorescent microscopic pictures of BGC-823 with GFP expression vector. (I) *Eag1* mRNA expression level in SGC-7901. (J) Eag1 protein expression level in SGC-7901. (K) *Eag1* mRNA expression level in BGC-823. (L) Eag1 protein expression level in BGC-823. The scale bar indicates 100 μm in A-H. mRNA, messenger RNA; shRNA, short hairpin RNA; GFP, green fluorescence protein.

and GraphPad Prism 5 software (GraphPad Software, San Diego, CA, USA). All statistical analyses were conducted with SAS 9.4 software (SAS Institute, Cary, NC, USA).

## Results

### Effects of shRNA treatment on Eag1 expression in GC cells

We analyzed the impact of shRNA transfection on mRNA and protein expression of *Eag1* in the shRNA vector, empty vector, and control groups. The transfection efficiency of Ad5-Eag1-shRNA in SGC-7901 and BGC-823 are shown in *Figure 1A-1H*. When compared with control group, the *Eag1* gene expression was downregulated by 55.7% in SGC-7901 and 68.3% in BGC-823 in the shRNA group. Similarly, the protein expression of Eag1 was significantly downregulated by 66.7% in the SGC-7901 and downregulated by 61.6%
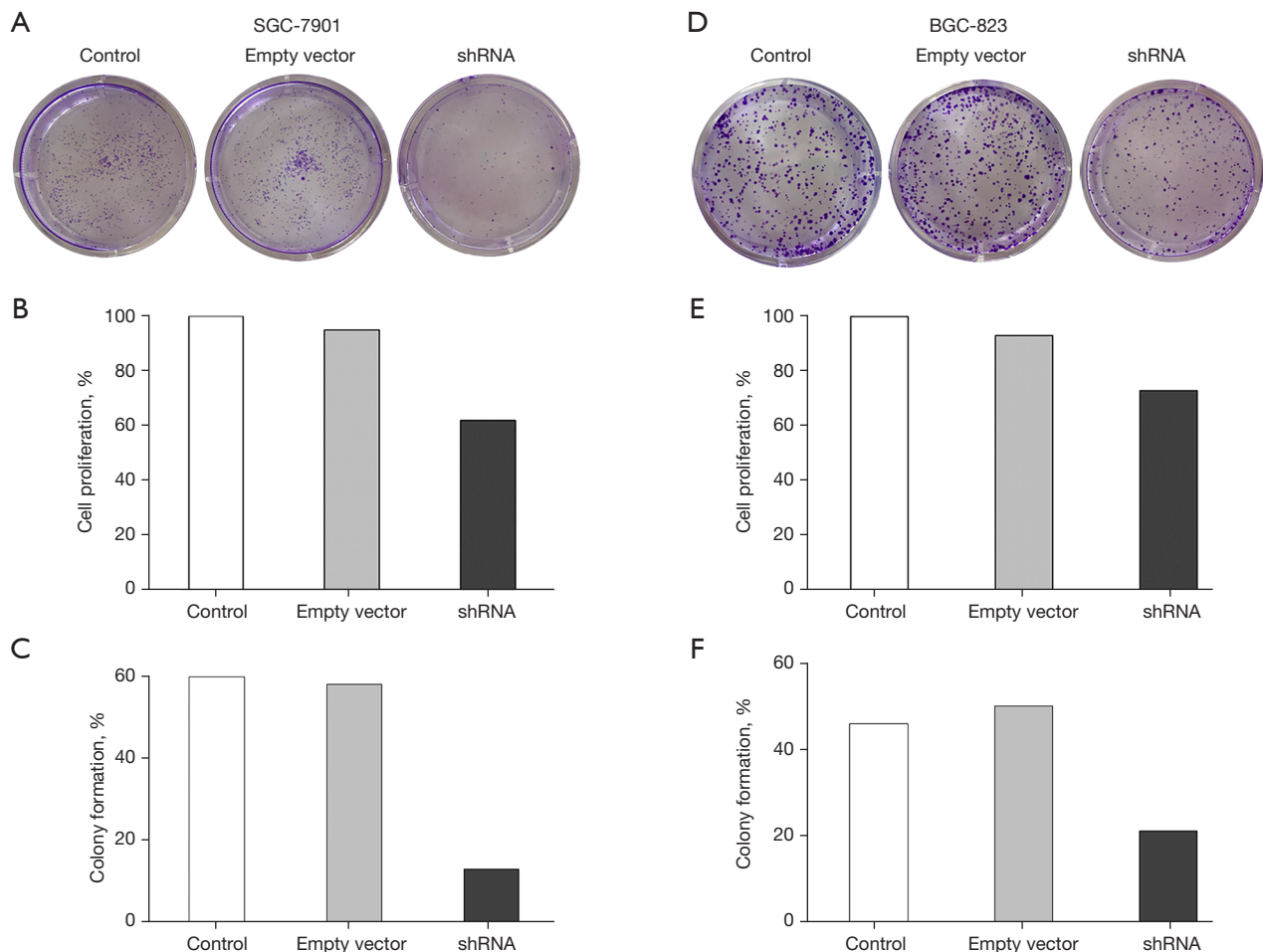
**Figure 2** Effects of transfection with Ad5-Eag1-shRNA on gastric cancer cell proliferation. (A) Transfection efficiency of Ad5-Eag1-shRNA in pictures of SGC-7901 (Giemsa staining, observed with camera). (B) Cell proliferation in different groups of SGC-7901. (C) Cell colony formation in SGC-7901. (D) Transfection efficiency of Ad5-Eag1-shRNA in pictures of BGC-823 (Giemsa staining, observed with camera). (E) Cell proliferation in different groups of BGC-823. (F) Cell colony formation in BGC-823. shRNA, short hairpin RNA.

in the BGC-823 transfected with shRNA vector compared to the control group (*Figure 1I-1L*). The same results were also observed between cell lines transfected with the shRNA vector and empty vector.

### Eag1 knockdown and cell proliferation

To estimate influence of transfection with Ad5-Eag1-shRNA on cell proliferation, CCK-8 was performed to analyze the rate of cell proliferation and colony formation in different cell groups. The transfection efficiency of Ad5-Eag1-shRNA on SGC-7901 cell proliferation is shown in *Figure 2A*. As shown in *Figure 2*, in comparison with the empty vector group and control group, the cell proliferation

rate was lower in SGC-7901 transfected with Ad5-Eag1-shRNA (all P<0.05) (*Figure 2B*). Moreover, the clone formation number in the shRNA group was decreased compared with the empty vector group and control group, and the differences were statistically significant in SGC-7901 cell lines (*Figure 2C*). Similar pictures were found in BGC-823 cell lines (*Figure 2D-2F*).

### Eag1 knockdown and cell cycle of GC

Flow cytometry was performed for the estimation of cell cycle progression as well as the effects of *Eag1* knockdown on GC cell cycle. *Figure 3* shows that compared with the control group, the cells transfected with Ad5-Eag1-shRNA
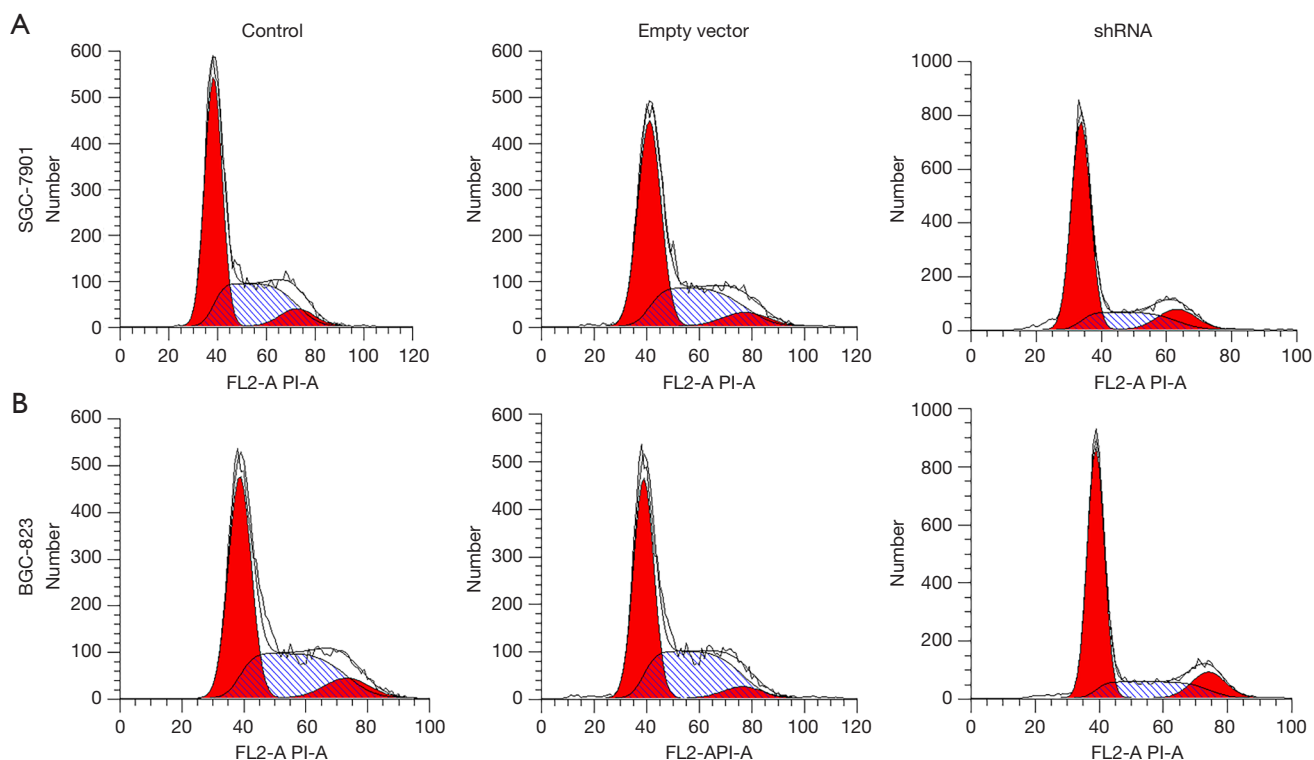
**Figure 3** Effects of *Eag1* knockdown on gastric cancer cell cycle. (A) SGC-7901 cell lines. (B) BGC-823 cell lines.

presented a cell cycle increase at $G_1$-$G_0$ phase (65.7% at 33.73 with shRNA vector *vs.* 55.5% at 38.25 with the control group for SGC-7901 and 64.8% at 38.89 with shRNA vector *vs.* 51.7% at 38.68 with the control group for BGC-823). Decreased $G_2$-S phase was also seen in the comparison between GC lines transfected with Ad5-Eag1-shRNA and the control group. Moreover, both SGC-7901 and BGC-823 in the shRNA group and empty vector showed a similar cell cycle effect (*Figure 3*).

### *Eag1 knockdown and cyclin D1/cyclin E expression in GC cells*

The influence of *Eag1* knockdown on protein expression of cyclin D1 and cyclin E was also evaluated. As shown in *Figure 4*, when GC cells were transfected with Ad5-Eag1-shRNA, cyclin D1 expression was inhibited by 66.3% in the SGC-7901 and 65.4% in the BGC-823 in comparison with control group. Similarly, protein expression of cyclin E was significantly downregulated by 64.8% in the SGC-7901 and downregulated by 74.8% in the BGC-823 transfected with the shRNA vector. The same results were also observed between cell lines transfected with shRNA vector and those

with the empty vector (*Figure 4*).

### *mRNA and protein expression validation*

The mRNA expression difference of *Eag1* in tumor samples and adjacent normal tissue samples were evaluated in TCGA database. The mRNA expression of *Eag1* was higher in tumor samples than in normal samples (0.21±0.12 *vs.* 0.13±0.08, P<0.001, *Figure 5A*). The same results were yielded in the difference analysis between tumor samples and adjacent normal samples (0.18±0.11 *vs.* 0.11±0.07, P<0.001, *Figure 5B*). Immunohistochemistry information of Eag1 in HPA indicated that the protein level of Eag1 was higher in tumor samples compared with normal samples (*Figure 5C,5D*).

### *Association between Eag1 expression and GC prognosis*

*Figure 6* shows the results of Kaplan-Meier survival analysis for subgroup analysis of *Eag1* gene expression level and GC prognosis, indicating that patients with higher *Eag1* expression may have a less favorable prognosis than overall GC and different characteristics patients (age, gender, M
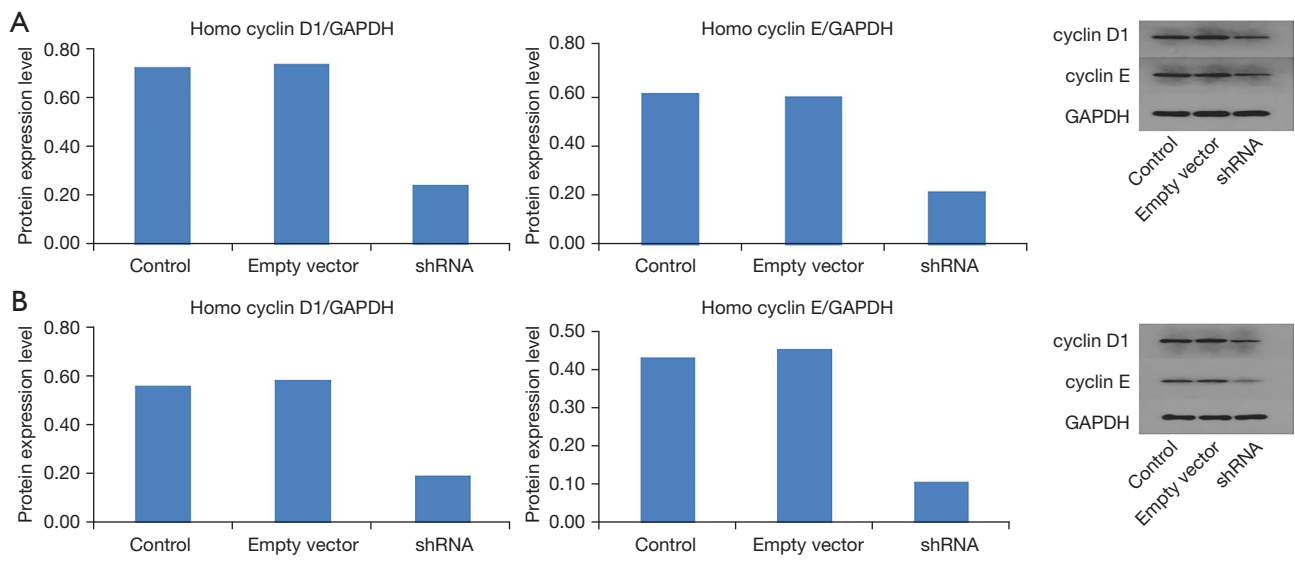
**Figure 4** Effects of *Eag1* knockdown on cyclin D1 and cyclin E protein expression in gastric cancer cells. (A) SGC-7901 cell lines. (B) BGC-823 cell lines.
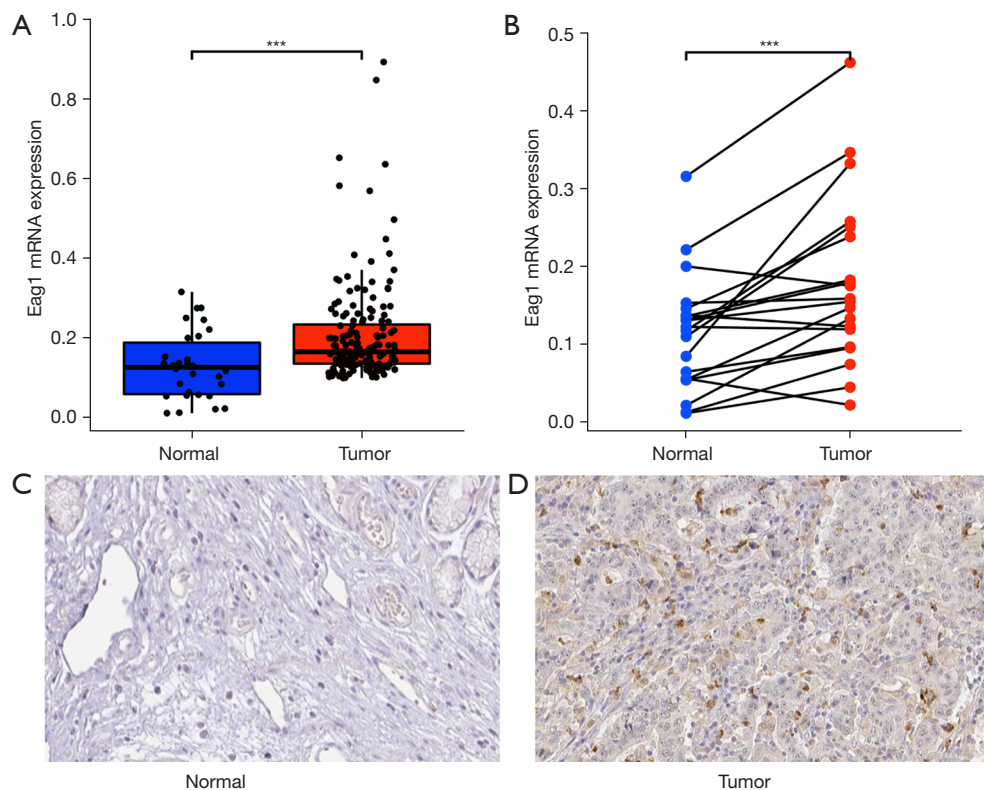


**Figure 5** *Eag1* mRNA and protein expression based on TCGA and HPA. (A,B) *Eag1* mRNA expression in gastric cancer sample and normal sample based on TCGA, Unpaired and paired. (C,D) Immunohistochemistry information of Eag1 in gastric cancer patients based on HPA, normal samples (image available from https://www.proteinatlas.org/ENSG00000143473-KCNH1/tissue/stomach#img), and tumor samples (image available from https://www.proteinatlas.org/ENSG00000143473-KCNH1/pathology/stomach+cancer#img). The scale bar indicates 100 μm in (C) and (D). ***P<0.001. mRNA, messenger RNA; HPA, Human Protein Atlas.
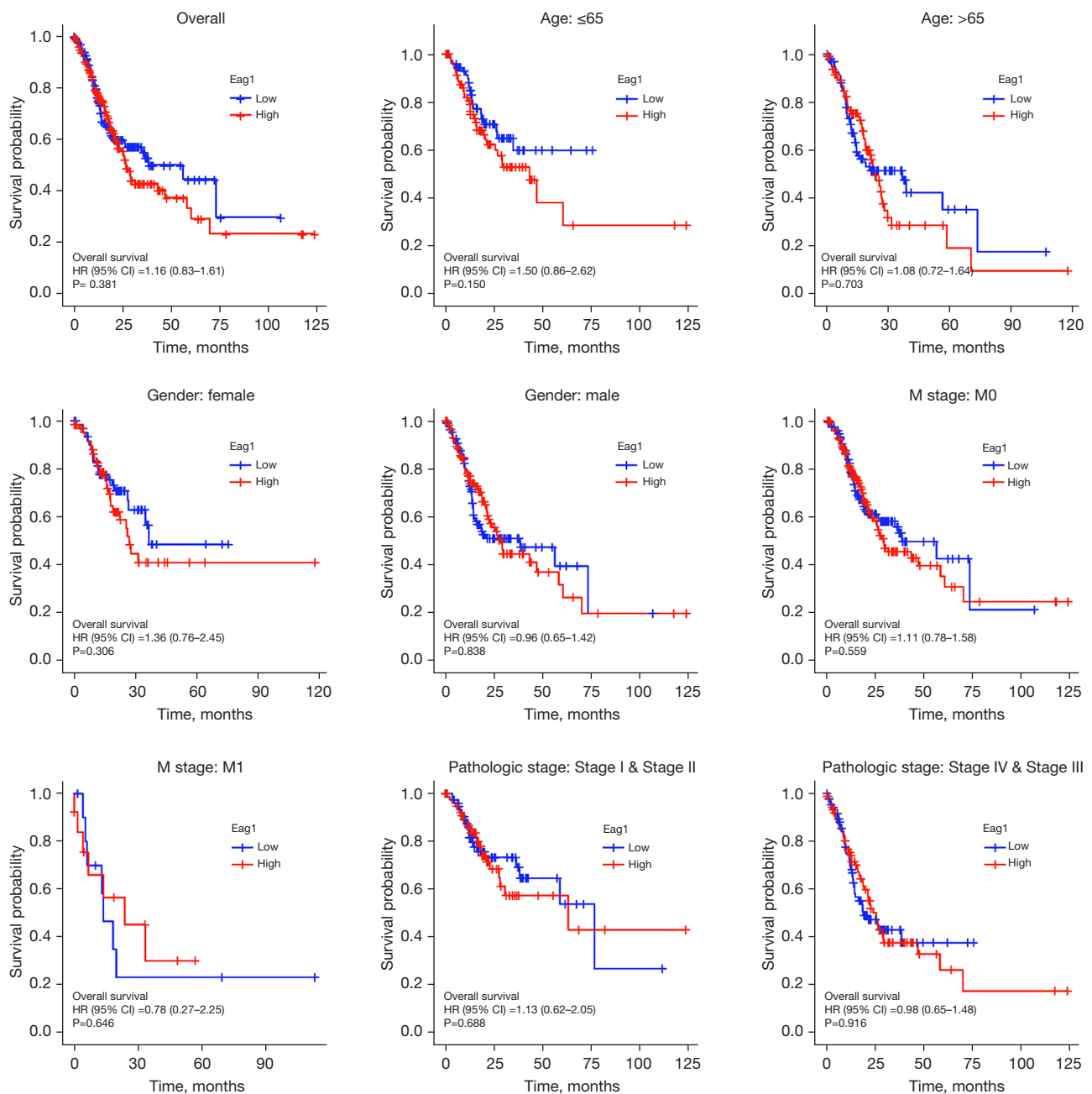
**Figure 6** Kaplan-Meier analysis of the association between *Eag1* expression and gastric cancer prognosis in subgroups. HR, hazard ratio; CI, confidence interval.

stage, pathologic stage, and so on).

A nomogram was further performed for GC prognosis with *Eag1* expression and some common clinicopathological variables according to the results of univariate Cox regression analysis (*Figure 7*). The 1-, 2-, and 3-year survival probability for GC patients was estimated by combining all the variables in the nomogram. The C-statistic value for nomogram verification was 0.814, suggesting that the nomogram has a satisfactory accuracy for prediction of GC prognosis.
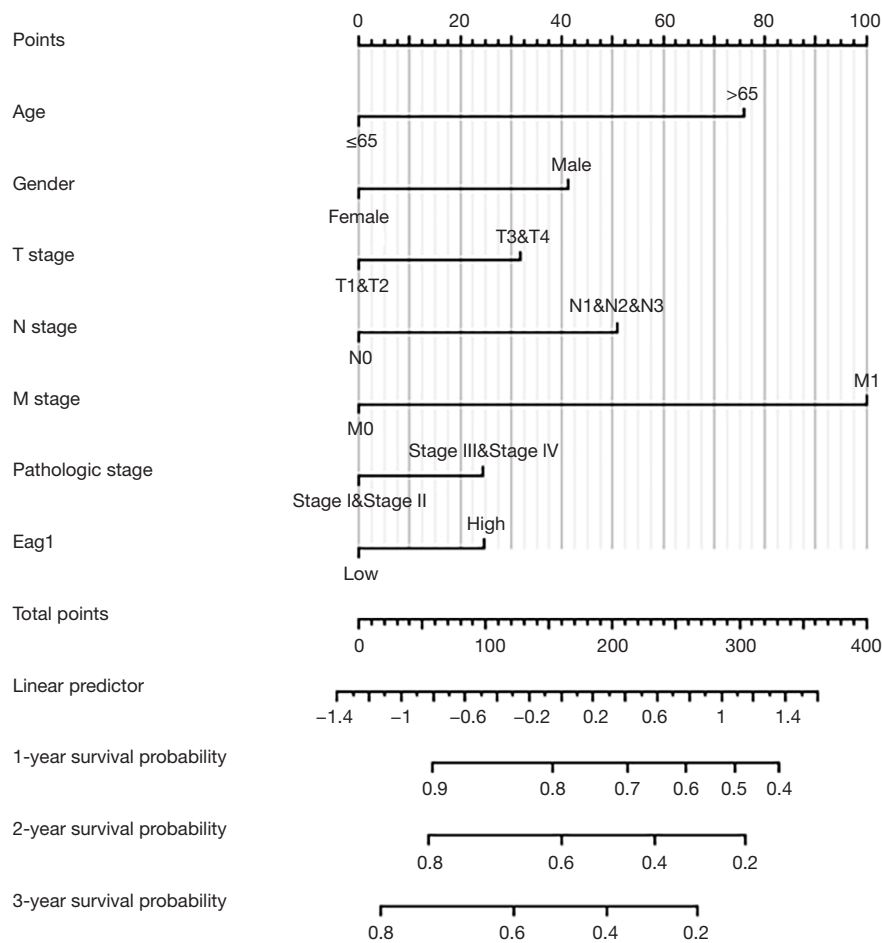
**Figure 7** Nomogram for the prediction of gastric cancer prognosis. T, tumor, N, node; M, metastasis.

### Functional enrichment analysis

Functional enrichment analysis was conducted for the DEGs of *Eag1*. Genes were divided into two groups with the median of *Eag1*, and the DEGs of *Eag1* were defined as: false discovery rate (FDR) <0.05 and |log₂ fold change| >1.5. Finally, 3,388 genes with 3,366 up-regulation genes and 22 down-regulation genes were identified, as shown in *Figure 8A*. *Figure 8B* displays the heatmap of the top 10 DEGs.

For enrichment analysis, GO and KEGG analyses were conducted for molecular biological functions evaluation (*Figure 8C,8D*). For the 3,388 DEGs of *Eag1*, the following BPs were enriched: keratinization, sensory perception of smell, and serotonin receptor signaling pathway. Also, the following CCs were enriched: intermediate filament and intermediate filament cytoskeleton. Lastly, the following MFs were enriched: olfactory receptor activity, G protein-coupled amine receptor activity, and neurotransmitter receptor activity.

### Relationship between Eag1 gene expression and status of immune infiltration

It has been reported that cancer-associated fibroblasts may have a crucial effect on the regulation of tumor infiltrating immune cells (17). In addition, considering the role of *Eag1* in actin cytoskeleton structure regulation, the relationship between *Eag1* gene expression and status of tumor immune infiltration was further estimated. The EPIC, MCP-counter, TIDE, and Xcell algorithms were employed to evaluate the correlation between *Eag1* expression and immune infiltration of cancer-associated fibroblast based on TCGA database, and *Eag1* gene expression was strongly related with the status of immune infiltration in
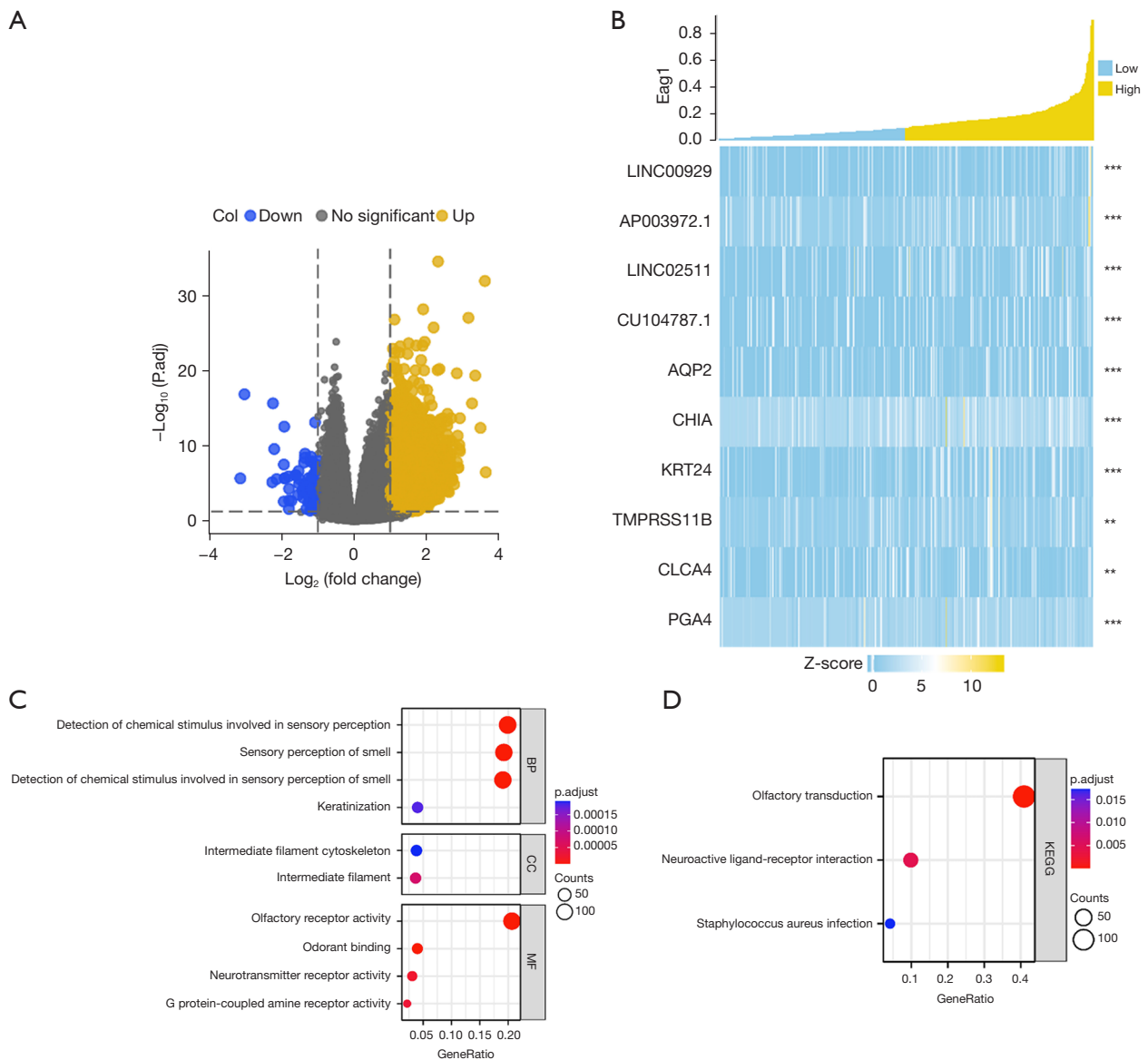
**Figure 8** Differential expression genetic map of *Eag1* in TCGA database. (A) Volcano plot. (B) Co-expression genes of *Eag1* (top10). (C) GO analysis. (D) KEGG analysis. **P<0.01, ***P<0.001. BP, biological process; CC, cellular component; MF, molecular function; TCGA, The Cancer Genome Atlas; GO, Gene Ontology; KEGG, Kyoto Encyclopedia of Genes and Genomes.

bladder cancer (BLCA), breast cancer (BRCA), stomach adenocarcinoma (STAD), and other tumors (*Figure 9*). We used TISIDB to estimate relationship between *Eag1* and status of immune infiltration in GC. It revealed that *Eag1* expression was significantly associated with abundance of Tcm-CD4+ T cell, CD56dim, neutrophils, macrophages, and other immune cells (all P<0.05, *Figure 9*).

## Discussion

In this study, according to functional experiment in vitro, we found that the gene and protein expression of *Eag1* was downregulated upon transfection with shRNA vector. Knockdown of *Eag1* inhibited the GC cell proliferation, whereas knockdown of *Eag1* decreased $G_2$-S phase cell
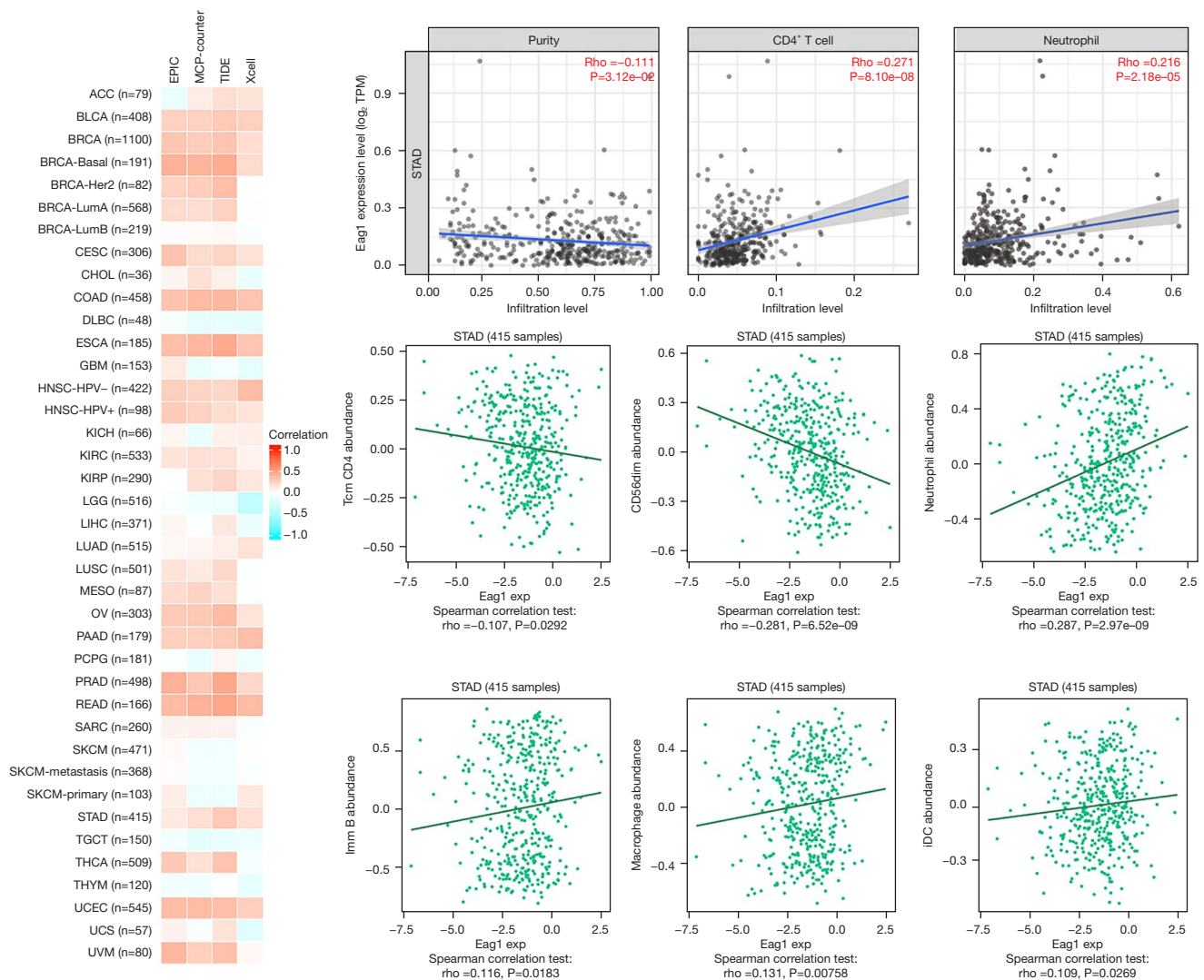
**Figure 9** Association between *Eag1* expression and gastric cancer infiltration. STAD, stomach adenocarcinoma; TPM, Transcripts Per Kilobase of exon model per Million mapped reads.

cycle progression. Our study estimated the influence of the *Eag1* channel on GC progression, indicating that *Eag1* knockdown can down-regulate cyclin D1 and cyclin E expression in vitro. This study suggests that the expression of *Eag1* may make a critical difference in the occurrence and progress of GC.

Bioinformatic analysis was also analyzed for *Eag1* validation with multiple public databases. Significant difference expression of *Eag1* gene and protein was observed between tumor samples and normal tissue samples. Kaplan-Meier survival analysis showed that *Eag1* expression was strongly related to GC prognosis; the nomogram indicated

a satisfied accuracy for prediction of GC prognosis. Enrichment analysis showed that *Eag1* and the DEGs can influence the regulation of intermediate filament, intermediate filament cytoskeleton, and G protein-coupled amine receptor activity. In addition, a significant correlation between *Eag1* expression and GC immune infiltration was seen based on TISIDB and TIMER.

As a kind of voltage-gated potassium channel, the *Eag* gene was first reported in 1969 and was shown to cause *Drosophila melanogaster* to move slowly and regularly under anesthesia (18). *Eag1* has been proved to be an important member of *Eag* subfamily, and can encode a member of

subfamily H, which can affect the normal physiological activity of potassium channels by regulating voltage gating (19). Pardo *et al.* confirmed the close relationship between *Eag1* and the development of tumors for the first time in 1999 (20). Several studies have shown that an abnormal expression state of *Eag1* in human tumor cell lines and tumor tissue can influence the proliferation, invasion, and other biological functions of tumor cells (21-23). This suggests that *Eag1* may be a useful tumor biomarker for therapy in different cancers. The *Eag1* channel consists of 6 transmembrane helices, including potassium selective pores and voltage sensors (24). Studies have shown that the voltage sensor in the *Eag1* channel may undergo structural changes and then regulate the channel switch when the membrane potential changes (25-27). As an *Eag1* channel inhibitor, astemizole may be a potential drug to restrain the proliferation of tumor cells because of its target proteins associated with cancer (28). Some studies have found that cell proliferation is blocked when measured with astemizole, suggesting that astemizole may play a crucial role in *Eag1* channel inhibition (29,30). A similar conclusion was obtained in an *in vivo* study (31). However, the role of the *Eag1* channel in possible biological mechanism of GC remains unclear.

This study showed *Eag1* expression may have a certain influence on the progression of GC through regulating cyclin D1 and cyclin E expression according to functional experiments. However, there are still limitations to the study. Only the effect of *Eag1* in GC development in tumor cell lines was considered. However, some studies have confirmed a strong relationship between *Eag1* expression and GC development in animal models (32,33). In consideration of the functional experimental results presented in this study, our findings still provide important information regarding the *Eag1* channel and the initiation and development of GC. Further studies, including experiments in animal models and human populations, are planned to validate the impact of *Eag1* on the development of and susceptibility to GC.

## Conclusions

In conclusion, this study found that the expression of *Eag1* may affect the initiation and occurrence of GC through regulating cyclin D1 and cyclin E expression. Further functional experiments including animal models and population studies with sufficient samples are necessary to verify our findings.

## Footnote

*Reporting Checklist*: The authors have completed the MDAR reporting checklist. Available at https://tcr.amegroups.com/article/view/10.21037/tcr-22-2276/rc

*Data Sharing Statement:* Available at https://tcr.amegroups.com/article/view/10.21037/tcr-22-2276/dss

*Conflicts of Interest*: All authors have completed the ICMJE uniform disclosure form (available at https://tcr.amegroups.com/article/view/10.21037/tcr-22-2276/coif). The authors have no conflicts of interest to declare.

*Ethical Statement*: The authors are accountable for all aspects of the work in ensuring that questions related to the accuracy or integrity of any part of the work are appropriately investigated and resolved. The study was conducted in accordance with the Declaration of Helsinki (as revised in 2013).

## References

1. Siegel RL, Miller KD, Fuchs HE, et al. Cancer Statistics, 2021. CA Cancer J Clin 2021;71:7-33.

2. Sung H, Ferlay J, Siegel RL, et al. Global Cancer Statistics 2020: GLOBOCAN Estimates of Incidence and Mortality Worldwide for 36 Cancers in 185 Countries. CA Cancer J Clin 2021;71:209-49.

3. Smyth EC, Nilsson M, Grabsch HI, et al. Gastric cancer. Lancet 2020;396:635-48.

4. Thrift AP, El-Serag HB. Burden of Gastric Cancer. Clin Gastroenterol Hepatol 2020;18:534-42.

5. Zhao Y, Zhang J, Cheng ASL, et al. Gastric cancer: genome damaged by bugs. Oncogene 2020;39:3427-42.

6. Docampo E, Martin M, Gangolf M, et al. Heredity and cancer. Rev Med Liege 2021;76:327-36.

7. Petryszyn P, Chapelle N, Matysiak-Budnik T. Gastric Cancer: Where Are We Heading? Dig Dis 2020;38:280-5.

8. Pardo LA, Stühmer W. Eag1: an emerging oncological target. Cancer Res 2008;68:1611-3.

9. Fang YC, Fu SJ, Hsu PH, et al. Identification of MKRN1 as a second E3 ligase for Eag1 potassium channels reveals regulation via differential degradation. J Biol Chem 2021;296:100484.

10. Lin H, Li Z, Chen C, et al. Transcriptional and post-transcriptional mechanisms for oncogenic overexpression of ether a go-go K+ channel. PLoS One 2011;6:e20362

11. Rodríguez-Rasgado JA, Acuña-Macías I, Camacho J. Eag1 channels as potential cancer biomarkers. Sensors (Basel) 2012;12:5986-95.

12. Ding XW, Luo HS, Jin X, et al. Aberrant expression of Eag1 potassium channels in gastric cancer patients and cell lines. Med Oncol 2007;24:345-50.

13. Li Z, Zhu K, Gong X, et al. Inducing Polyclonal Eag1-Specific Antibodies by Vaccination with a Linear Epitope Immunogen and Its Relation to Breast Tumorigenesis. Pathol Oncol Res 2017;23:761-7.

14. Pardo LA, Contreras-Jurado C, Zientkowska M, et al. Role of voltage-gated potassium channels in cancer. J Membr Biol 2005;205:115-24.

15. Chen J, Xuan Z, Song W, et al. EAG1 enhances hepatocellular carcinoma proliferation by modulating SKP2 and metastasis through pseudopod formation. Oncogene 2021;40:163-76.

16. Chávez-López MG, Zúñiga-García V, Castro-Magdonel BE, et al. Eag1 Gene and Protein Expression in Human Retinoblastoma Tumors and its Regulation by pRb in HeLa Cells. Genes (Basel) 2020;11:119.

17. Chen X, Song E. Turning foes to friends: targeting cancer-associated fibroblasts. Nat Rev Drug Discov 2019;18:99-115.

18. Kaplan WD, Trout WE 3rd. The behavior of four neurological mutants of Drosophila. Genetics 1969;61:399-409.

19. Wang X, Chen Y, Li J, et al. Tetrandrine, a novel inhibitor of ether-à-go-go-1 (Eag1), targeted to cervical cancer development. J Cell Physiol 2019;234:7161-73.

20. Pardo LA, del Camino D, Sánchez A, et al. Oncogenic potential of EAG K(+) channels. EMBO J 1999;18:5540-7.

21. Toplak Ž, Hendrickx LA, Abdelaziz R, et al. Overcoming challenges of HERG potassium channel liability through rational design: Eag1 inhibitors for cancer treatment. Med Res Rev 2022;42:183-226.

22. Asher V, Khan R, Warren A, et al. The Eag potassium channel as a new prognostic marker in ovarian cancer. Diagn Pathol 2010;5:78.

23. Shi Y, Yang X, Xue X, et al. HANR promotes lymphangiogenesis of hepatocellular carcinoma via secreting miR-296 exosome and regulating EAG1/VEGFA signaling in HDLEC cells. J Cell Biochem 2019;120:17699-708.

24. Whicher JR, MacKinnon R. Regulation of Eag1 gating by its intracellular domains. Elife 2019;8:49188.

25. Wynia-Smith SL, Gillian-Daniel AL, Satyshur KA, et al. hERG gating microdomains defined by S6 mutagenesis and molecular modeling. J Gen Physiol 2008;132:507-20.

26. Thouta S, Sokolov S, Abe Y, et al. Proline scan of the HERG channel S6 helix reveals the location of the intracellular pore gate. Biophys J 2014;106:1057-69.

27. Wang X, Chen Y, Liu H, et al. A novel anti-cancer mechanism of Nutlin-3 through downregulation of Eag1 channel and PI3K/AKT pathway. Biochem Biophys Res Commun 2019;517:445-51.

28. García-Quiroz J, Camacho J. Astemizole: an old anti-histamine as a new promising anti-cancer drug. Anticancer Agents Med Chem 2011;11:307-14.

29. Gómez-Varela D, Zwick-Wallasch E, Knötgen H, et al. Monoclonal antibody blockade of the human Eag1 potassium channel function exerts antitumor activity. Cancer Res 2007;67:7343-9.

30. de Guadalupe Chávez-López M, Pérez-Carreón JI, Zuñiga-García V, et al. Astemizole-based anticancer therapy for hepatocellular carcinoma (HCC), and Eag1 channels as potential early-stage markers of HCC. Tumour Biol 2015;36:6149-58.

31. Ufartes R, Schneider T, Mortensen LS, et al. Behavioural

and functional characterization of Kv10.1 (Eag1) knockout mice. Hum Mol Genet 2013;22:2247-62.

32. Asher V, Sowter H, Shaw R, et al. Eag and HERG potassium channels as novel therapeutic targets in cancer. World J Surg Oncol 2010;8:113.

33. Weber C, de Queiroz FM, Downie BR, et al. Silencing the activity and proliferative properties of the human EagI Potassium Channel by RNA Interference. J Biol Chem 2006;281:13030-7.